Solution Structure of Glutathione Bound to Human Glutathione Transferase P1-1: Comparison of NMR Measurements with the Crystal Structure†

Maria Nicotra,‡ Maurizio Paci,§ Marco Sette,§ Aaron J. Oakley,|| Michael W. Parker,|| Mario Lo Bello,‡ Anna Maria Caccuri,‡ Giorgio Federici,⊥ and Giorgio Ricci*,‡

Department of Biology, University of Rome "Tor Vergata", Via della Ricerca Scientifica 00133 Rome, Italy, Department of Chemical Sciences, University of Rome "Tor Vergata", Via della Ricerca Scientifica 00133 Rome, Italy, The Ian Potter Foundation Protein Crystallography Laboratory, St. Vincent's Institute of Medical Research, 41 Victoria Parade, Fitzroy, Victoria 3065, Australia, and Osp. Pediatrico IRCCS "Bambin Gesù", 00165 Rome, Italy

Received August 4, 1997; Revised Manuscript Received December 11, 1997

ABSTRACT: The conformation of the bound glutathione (GSH) in the active site of the human glutathione transferase P1-1 (EC 2.5.1.18) has been studied by transferred NOE measurements and compared with those obtained by X-ray diffraction data. Two-dimensional TRNOESY and TRROESY experiments have been performed under fast-exchange conditions. The family of GSH conformers, compatible with TRNOE distance constraints, shows a backbone structure very similar to the crystal model. Interesting differences have been found in the side chain regions. After restrained energy minimization of a representative NMR conformer in the active site, the sulfur atom is not found in hydrogen-bonding distance of the hydroxyl group of Tyr 7. This situation is similar to the one observed in an "atypical" crystal complex grown at low pH and low temperature. The NMR conformers display also a poorly defined structure of the glutamyl moiety, and the presence of an unexpected intermolecular NOE could indicate a different interaction of this substrate portion with the G-site. The NMR data seem to provide a snapshot of GSH in a precomplex where the GSH glutamyl end is bound in a different fashion. The existence of this precomplex is supported by pre-steady-state kinetic experiments [Caccuri, A. M., Lo Bello, M., Nuccetelli, M., Nicotra, M., Rossi, P., Antonini, G., Federici, G., and Ricci, G. (1998) *Biochemistry 37*, 3028−3034] and preliminary time-resolved fluorescence data.

Cytosolic glutathione transferases (EC 2.5.1.18; GSTs)[1] are a family of dimeric enzymes able to conjugate the natural tripeptide glutathione (GSH, γ−L-glutamyl-L-cysteinyl-glycine) to dangerous endogenous or xenobiotic compounds which contain an electrophilic center (*1*). They have been grouped into at least five gene-independent classes named Alpha, Mu, Pi, Theta, and Sigma (*2*−*5*). The three-dimensional crystal structures of representative isoenzymes of each class in complex with GSH or GSH derivatives show very similar tertiary architecture and quite identical geometry of the substrate bound in the active site (G-site) (*6*−*11*). These crystallographic data provide the picture of a ligand−enzyme complex in a frozen state, but the scenario could be more complicated in solution. In fact, several regions of the protein are quite flexible; for example, motions of the irregular α-helix 2 (residues 35−46) which forms part of the G-site, modulate the kinetic parameters of this enzyme and are also involved in an induced fit mechanism upon GSH binding (*12*). The latter structural arrangement can be explained by assuming that the binding process of a flexible ligand to a flexible enzyme is the result of the reciprocal selection of one (or a few) among the many interconverting conformers both of the substrate and of the enzyme. Alternatively, a reciprocal structural modeling may occur after a first precomplex formation. A detailed knowledge of the GSH binding process is important for drug design purposes, since this isoenzyme is involved in the mechanism of cellular multidrug resistance against a number of chemotherapeutic agents (*13*−*15*). In this paper, we compare the structure of GSH in complex with GST P1-1 with that observed in solution by transferred NOE measurements. The

† M.W.P. is an Australian Research Council Senior Research Fellow and A.J.O. was a recipient of a National Health & Medical Research Council Postgraduate Research Scholarship and an International Centre for Diffraction Data Crystallography Scholarship. We gratefully acknowledge the financial support of the Anti-Cancer Council of Victoria and of the Italian National Council of Research, Progetto Finalizzato ACRO and Progetto Strategico "Biologia Strutturale". This work was also partially supported by a grant of Ministero dell'Università e della Ricerca Scientifica e Tecnologica (funds 40% and 60%).

* Address for correspondence: Department of Biology, University of Rome "Tor Vergata", Viale della Ricerca Scientifica, 00133 Rome, Italy. Tel: +39+6+72594375. Fax: +39+6+2025450. E-mail: ricci@utovrm.it.

‡ Department of Biology, University of Rome "Tor Vergata".

§ Department of Chemical Sciences, University of Rome "Tor Vergata".

|| St. Vincent's Institute of Medical Research.

⊥ Osp. Pediatrico IRCCS "Bambin Gesù".

[1] Abbreviations. DG-SA, distance geometry-simulated annealing; DTT, dithiothreitol; EDTA, ethylenediaminetetracetic acid; GSH, glutathione (γ-L-glutamyl-L-cysteinyl-glycine); GST, glutathione transferase; NMR, nuclear magnetic resonance; NOE, nuclear Overhauser effect; NOESY, nuclear Overhauser effect spectroscopy; rmsd, root-mean-square deviation; TRNOE, transferred NOE; TRNOESY, transferred NOESY; ROE, rotating-frame nuclear Overhauser enhancement; ROESY, rotating-frame nuclear Overhauser enhancement spectroscopy; TRROE, transferred ROE; TRROESY, transferred ROESY; TOCSY, total correlation spectroscopy; TPPI, time proportional phase increment.

S0006-2960(97)01902-8 CCC: $15.00
Published on Web 02/12/1998

TRNOE procedure has been used extensively to determine the conformation of small ligands bound to macromolecules (for review, see ref *16*) and it may provide useful details about the early stage of the substrate binding. In the absence of GST P1-1, the GSH molecule displays a large conformational flexibility in solution and no preference for any particular conformation (*17*). Transferred NOE data, obtained in the presence of catalytic amounts of GST P1-1 and under fast exchange conditions, indicate that the interaction with the active site produces a freezing of the bound GSH in a restricted region of the conformational space. Distance geometry and simulated annealing algorithms allowed us to obtain a number of conformations for the bound GSH compatible with the NOE data. The extended backbone of these conformers is similar to that found in the crystal complex. Notable differences concern the spatial geometry of the Cys side chain and the interaction of the glutamyl moiety with the G-site. These findings are discussed taking into account that GSH binding follows a multistep binding mechanism and the solution is mainly populated by GSH molecules which retain the magnetization of a weakly bound precomplex.

EXPERIMENTAL PROCEDURES

Sample Preparation. GSH was purchased from Sigma and used without further purification. GST P1-1 was expressed in *Escherichia coli* and purified as described previously (*18*). NMR samples for TOCSY, NOESY, and ROESY experiments contained 4 mM of GSH in H_2O (in the presence of 20% D_2O, 0.1 M KH_2PO_4, 0.1 M KCl, 0.1 mM EDTA, and 0.2 mM DTT, pH 5.2) with or without GST P1-1. Molar ratios substrate:enzyme were 5:1 and 10:1. The presence of DTT is necessary to prevent any spontaneous oxidative process involving protein cysteines (*19*).

NMR Spectroscopy. NMR spectra were obtained at 25 °C on a Bruker AM 400 instrument operating at 400.13 MHz. Two-dimensional NMR experiments were performed in the phase sensitive mode with TPPI phase cycle (*20*) typically using 2K of memory for 512 increments. The number of scans was optimized in order to obtain a satisfactory signal-to-noise ratio. Correlation experiments were carried out as total correlation (TOCSY) where the MLEV-17 spinlock composite pulse sequence has been inserted (*21*, *22*) with a typical mixing time of either 16 or 64 ms in order to observe either direct or both direct and remote connectivities. NOE dipolar correlated two-dimensional spectra were obtained using the NOESY pulse sequence (*23*). The mixing time for the magnetization exchange ranged within 100−300 ms. Rotating frame dipolar correlated 2D spectroscopy (ROESY) was performed accordingly to Bothner-By (*24*) and Griesinger and Ernst (*25*). The mixing times for the magnetization exchange were 50, 80, 155, and 225 ms.

Data were processed on a microVax II with the TRITON two-dimensional NMR software from license of the University of Utrecht, The Netherlands. Free induction decays were weighted by a sinebell apodization function shifted typically $\pi/3$ in both dimensions. In all homonuclear two-dimensional experiments, a matrix 1024 × 1024 in the phase sensitive mode was thus obtained with a digital resolution of about 5 Hz/point. A baseline correction was made in both dimensions using a polynomial fit routine present in the same program.

Structure Determination. For the structure determination, a hybrid distance geometry-simulated annealing (DG-SA) protocol was carried out using the program X-PLOR 3.1 (*26*). The topology of GSH required the insertion of the peculiar γ-glutamyl-cysteinyl peptide bond. NOE-derived distance constraints were classified as strong, medium, and weak and translated into upper bounds of 2.7, 3.3, and 4.0 Å, respectively; a pseudoatom was introduced at the center of mass of the two equivalent methylene Cα protons of Gly, Cβ protons of Cys, Cγ and Cβ protons of Glu and a distance correction term of 0.3, 0.5, and 1.0 Å was added to the upper limit for strong, medium, and weak signals, respectively. The X-PLOR calculation to generate 50 three-dimensional structures of GSH was performed in two stages: the first one was 1 ps of Verlet dynamics at 2000 K to correct distance violation, and the second stage was cooling at 100 K in 50 K steps for final refinement followed by Powell minimization.

The 50 structures generated by distance geometry-simulated annealing protocol (DGSA-GSH) were checked on the basis of potential energy values and relevant NOE distance constraint violations (higher than 0.5 Å) and 20 discarded. The 30 selected structures were grouped in two families (A and B) on the basis of the homogeneity of dihedral angles and the rmsd pairwise values for backbone atoms. Family A shows zero NOE violations and Family B has some NOE violations $\leq$0.5 Å.

Molecular Modeling. Molecular modeling and energy minimization in the active site were performed with INSIGHT II version 2.3.0 and DISCOVER version 2.9.5 software packages (Molecular Simulation Inc., San Diego, CA) on a Silicon Graphics Personal Iris Workstation. The coordinates of the small cell C2 complex determined by crystallography (*27*) were used for the molecular modeling study. Hydrogens were built onto heavy atoms using the INSIGHT II program. A selected structure of family A (DGSA-GSH1), which shows an intermediate rmsd value for backbone atoms in respect to the crystal GSH model and also with a very low energy value, was modeled into the crystallographic binding site. It was initially positioned to overlay the backbone of GSH in the normal crystal complex. The protein coordinates were held fixed and the following protocol of energy minimization was performed: the first stage of minimization involved 300 cycles of steepest descent unrestrained minimization followed by 100 cycles of steepest descent and 1000 steps of conjugate gradient restrained minimization. CVFF force field and a distance-dependent dielectric constant $\epsilon = 4rij$ were used. A cutoff of 18 Å with a switching distance of 1.5 Å was employed for nonbonded interactions. The force constants for the NOE distance constraints were set at 50 kcal mol^{-1} Å^{-2}. The same procedure of minimization was applied to DGSA-GSH1 after forced deprotonation of the −SH group.

RESULTS

Conformation of the Bound GSH in the Crystal Complex. The crystal structure of human GST P1-1 in complex with GSH has been determined in three different crystal forms (*27*). In the C2 space group, the model has been refined to a resolution of 1.9 Å with a conventional *R*-factor of 20.0% (R_{free} = 21.8%). In the $P2_12_12_1$ space group, the model has

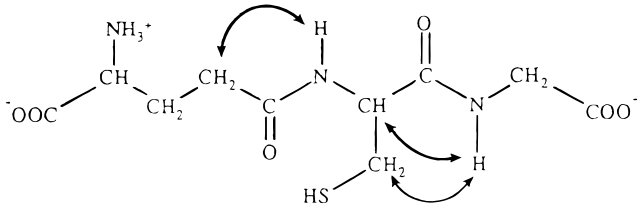

GSH

FIGURE 1: Chemical structure of GSH. Relevant proton−proton intramolecular interactions as derived by TRNOESY spectrum in the presence of substoichiometric amount of GST P1-1 are indicated by arrows. The thin arrow indicates a medium NOE while the two thick arrows represent strong NOEs.

been refined to a resolution of 2.2 Å with a conventional *R*-factor of 21.8% (R_{free} = 25.9%). In the big cell C2 form, the model has been refined to a resolution of 1.9 Å with a conventional *R*-factor of 19.3% (R_{free} = 22.9%).

The small cell C2 and $P2_12_12_1$ models show an identical GSH structure which also superimposes well on the extended conformation observed previously in GSH conjugate complexes to human GST P1-1 such as the *S*-hexylglutathione (*9*, *27*, *28*) and ethacrynic−GSH complexes (*29*). Furthermore, the same conformation has been observed in the crystal structures of numerous other GST complexes (*6*, *7*, *10*, *11*, *30*−*38*). In the human GST P1-1, GSH binds in extended fashion (Figure 3 and Tables 2 and 3) with the γ-glutamyl arm pointing downward into the core of the protein and toward the dimer interface whereas the glycyl arm points toward bulk solvent. Both of these arms form a number of interactions with the enzyme (*9*). The sulfur atom of the cysteinyl moiety is within hydrogen bonding distance of the hydroxyl group of Tyr 7 (Table 4), and it exists predominantly in the thiolate form (*39*, *40*). Throughout this paper, the small C2 cell and $P2_12_12_1$ cell are termed "normal" crystal complexes. In the big cell C2 model (termed "atypical" crystal complex), the GSH conformer is very similar to that found in the small C2 and $P2_12_12_1$ crystals (rmsd for the backbone = 0.17), with the exception that the direct hydrogen bonding interaction between Tyr 7 and GSH is broken and a water molecule mediates the interaction. The big cell C2 crystals have only been observed at low pH (5.4−6.0) and at low temperature (4 °C) whereas the data obtained from the other forms were based on crystals grown at higher pH (5.8−6.4) and at room temperature. We hypothesize that the source of the difference is that the GSH molecule in the big cell C2 form has crystallized in the un-ionized form whereas in the other complexes it has crystallized in the thiolate form.

Conformation of the Bound GSH Determined by TRNOE. The chemical structure of GSH is shown in Figure 1. The monodimensional ^{1}H NMR spectrum (not shown) of 4 mM GSH in H_2O in the presence of 20% D_2O, 0.1 M KH_2PO_4, 0.1 M KCl, 0.1 mM EDTA, and 0.2 mM DTT, pH 5.2, overlaps those reported previously under slightly different conditions (*41*). Resonance assignments are reported in Table 1.

The NOESY spectrum of GSH alone at different mixing times revealed the absence of dipolar connectivities. The total lack of NOESY cross-peaks may be a correlation time effect and should not reflect a molecular flexibility of the free GSH. However, at pH 5.3, the tripeptide was shown to be a dynamic ensemble of rapidly interconverting conformations (*17*). Addition of substoichiometric amount of GST P1-1 produces the appearance of 11 NOEs with negative intensities and the broadening of the resonances (Table 2). On the basis of the thermodynamic dissociation constant for the GSH-GST P1-1 complex ($K_D \cong 5 \times 10^{-5}$ M) (*42*) and on the assumption of a diffusion controlled *on* rate of GSH (about 10^8 s^{-1} M^{-1}), it results that the apparent k_{off} is much faster than the cross-relaxation rate of GSH bound ($\sigma_{3.0Å}$ = 0.7 s^{-1}) and therefore the fast-exchange condition may be assumed for TRNOE analysis (*43*, *44*). In Figure 2A, a selected region of the NOESY spectrum obtained at 10:1 GSH:enzyme molar ratio and at mixing times of 225 ms is reported. All the 11 NOEs were observed in the mixing time range of 100−300 ms and at both 10:1 and 5:1 GSH:enzyme molar ratios. The most relevant intramolecular proton−proton interactions are indicated by arrows in the molecular structure of GSH shown in Figure 1. The possibility of protein-mediated spin diffusion contributing to the GSH transferred NOE spectra has been evaluated by comparing TRNOESY and TRROESY data. In the TRROESY spectra, obtained in the presence of GST P1-1 and with mixing times ranging between 50 and 225 ms, all intraligand cross-peaks observed in the TRNOESY spectra are still present as positive peaks, thus excluding indirect interactions on the TRNOESY spectra (see Figure 2B) (*45*, *46*). The lack of intermolecular cross-peaks in TRROESY spectra is likely due to the fast relaxation (short $T_1\rho$) of protein resonances during the spinlock period. This leads to a disappearance of intermolecular NOEs besides to a decrease of sensitivity of ROESY pulse sequence (*16*).

ROESY reference spectra for the free GSH have been recorded at 155 and 225 ms of mixing time. These ROESY spectra are qualitatively similar to the TRROESY spectra. Quantitative analysis shows, however, that the relative intensities of the ROE peaks differ from the ones of the TRROE peaks (data not shown). This indicates a selective change of the relative populations of the GSH conformers likely due to a specific interaction with the enzyme.

In the TRNOESY spectra, three intermolecular NOEs are also detectable. The first one reveals a short distance between the CαH of Gly or Glu of GSH and a proton of a protein residue with a chemical shift of 7.35 ppm (Figure 2A, indicated by arrow). A second strong intermolecular NOE is due to the interaction of CβH of Glu with an enzyme proton at 4.0 ppm (not shown). The third strong NOE indicates an interaction between CβH of Cys and a protein proton at 1.23 ppm (not shown). These intermolecular NOEs will be discussed in the next section. The intensities of intramolecular NOEs observed in the NOESY spectrum were converted into distances and used to generate 50 three-dimensional GSH structures by the distance geometry-simulated annealing procedure (DGSA-GSH) as reported in the Experimental Section. Thirty of these structures were selected on the basis of the total energy evaluation and of zero or no relevant NOE distance violations (below 0.5 Å). By considering both the homogeneity of the dihedral angles and pairwise rmsd values, these conformations were grouped into two families. Family A is formed by 17 GSH conformers with zero NOE violations and a similar backbone structure which also overlaps well that observed in the three

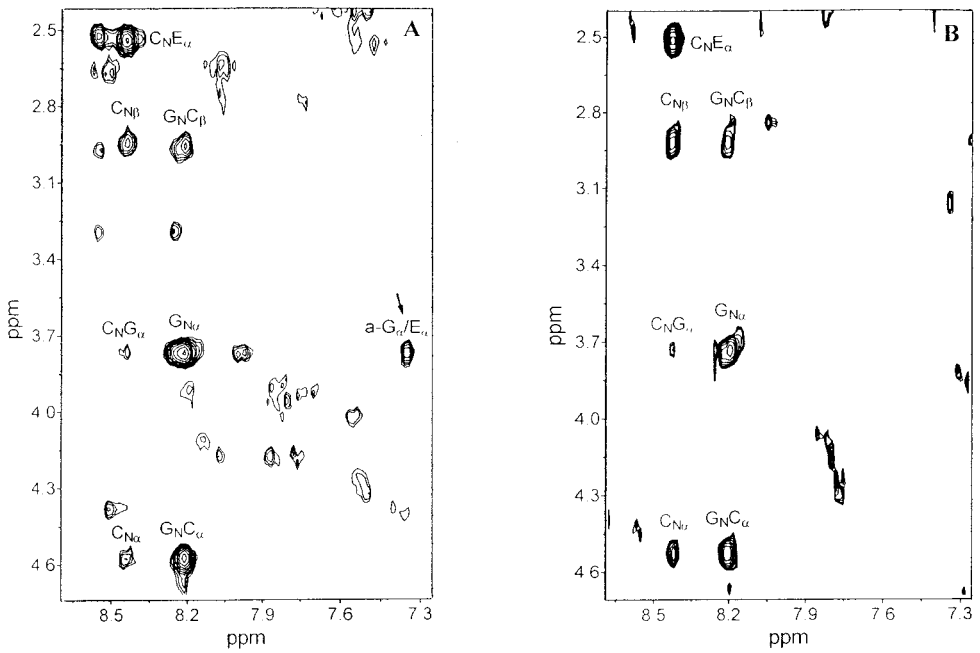

FIGURE 2: Comparison between a selected region of the two-dimensional NOESY and ROESY spectra of GSH bound to GST P1-1 at 400 MHz. GSH and enzyme concentrations were 4 and 0.4 mM, respectively (pH 5.2). Assay conditions are reported under Experimental Procedures. (A) TRNOESY spectrum obtained at a mixing time of 225 ms; the arrow indicates the intermolecular interaction between the CαH proton of Gly or Glu (see Discussion for final assignment) and a proton of the enzyme at 7.35 ppm. (B) TRROESY spectrum obtained at a mixing time of 80 ms. The lack of the intermolecular interaction at 3.76−7.35 ppm is discussed in the text.

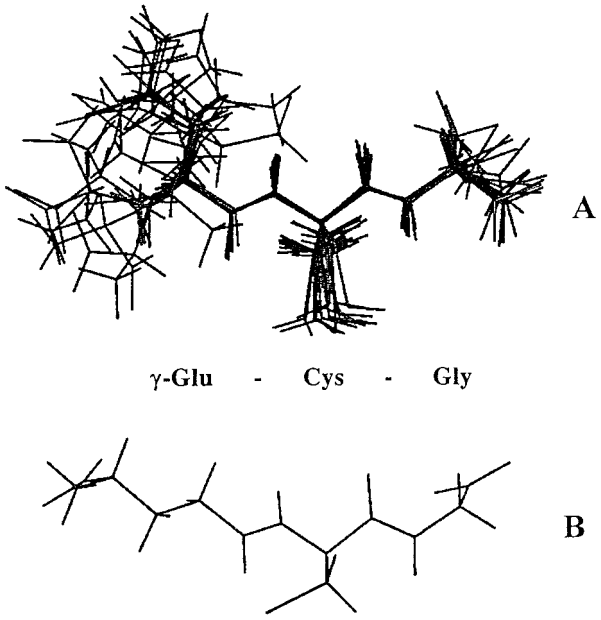

FIGURE 3: (A) Superposition of 17 calculated structures (family A) for GSH bound to GST P1-1 obtained from the hybrid distance geometry-simulated annealing procedure as described in Experimental Procedures. (B) GSH structure in the normal crystal complex (small cell C2 form).

Table 1: Proton Resonance Assignments of GSH (γ-L-Glu-L-Cys-Gly) in the Presence of GST P1-1 (4:0.4 mM), at pH 5.2

residue	proton	ppm
Glu	NH	
	CαH	3.76
	Cβ H	2.15
	Cγ H	2.53
Cys	NH	8.44
	CαH	4.56
	Cβ H	2.94
Gly	NH	8.22
	CαH	3.76

crystal structures (Table 3). The mean value of pairwise rmsd for the backbone atoms is 0.17 Å, comparing the individual structures, and 0.26 Å when each structure is compared to the normal crystal model. Family B contains 13 conformers which show some small NOE violations and a backbone structure quite different from the crystallographic one (the mean value of pairwise rmsd for backbone atoms compared to the crystal model is 0.75 Å). Due to NOE violations and to the large difference with the crystallographic GSH model, family B was not considered as a useful basis for further discussion. Family A conformers are shown in Figure 3, together with the structure of GSH as observed in the normal crystal GST−GSH complex. Family A conformers display a rather frozen backbone; on the contrary, the glutamyl moiety is poorly defined. By comparing family A structures with the normal crystal model, it is evident that the orientation of the sulfhydryl group of Cys is quite different ($\chi_{cys} = -124 \pm 15°$ and $\chi_{cys} = -46°$, respectively, see Table 3). A selected minimum energy GSH conformer (DGSA-GSH), which also displays an intermediate rmsd value in respect to the GSH molecule found in the normal crystal form, was modeled into the crystallographic G-site and initially positioned to overlay the backbone of the crystal GSH structure. In this initial condition, the sulfur atom, which is in the un-ionized form, is at 4.3 Å distance from the oxygen atom of Tyr 7 (S−H−O angle = 119°) (Table 4 and Figure 4). After restrained energy minimization procedure, the sulfur atom of this conformer (EMAS-GSH) is 4.0 Å distant from the oxygen atom of Tyr 7 (S−H−O angle = 121°) (Table 4 and Figure 4). In both cases, the O−S distance and the S−H−O angle are unfavorable for the hydrogen bond interaction. Moreover, the O−S distance and

Table 2: Distance Restraints from TRNOE Experiments Used for GSH Structure Determination in Comparison to Distances[a] Observed in the Normal Crystal Structure (Small Cell C2)

intraresidue				interresidue			
protein pair	distance restraints	strength[b]	distances in the crystal structure	protein pair	distance restraints	strength[b]	distances in the crystal structure
Glu1				Glu1−Cys2			
CαH−Cβ H	1.7−3.0	s	2.65	Cγ H−NH	1.7−3.0	s	2.25
CαH−Cγ H	1.7−3.0	s	2.70				
Cβ H−Cγ H	1.7−3.0	s	2.58				
Cys2				Cys2−Gly3			
CαH−Cβ H	1.7−3.8	m	2.56	NH−CαH	1.7−5.0	w	5.27
NH−CαH	1.7−3.3	m	3.16	CαH−NH	1.7−2.7	s	2.3
NH−Cβ H	1.7−3.8	m	3.26	Cβ H−NH	1.7−3.8	m	3.16
Gly3							
NH−CαH	1.7−3.0	s	2.61				

[a] Distances are reported in angstroms. Pseudoatoms were used for equivalent protons. [b] Classification of NOEs was s, strong; m, medium; and w, weak.

Table 3: Comparison between Selected Dihedral Angles (deg) in the GSH Molecule Observed in Family A Conformers and in the Crystal Structure

	NMR structures (family A)	normal crystal structure
$p\psi_{GLU}$ (CB1, CG1, CD1, N2)	-75 ± 37, 70 ± 35, 170 ± 13	−178
φ_{CYS} (CD1, N2, CA2, C2)	-165 ± 31	−134
ψ_{CYS} (N2, CA2, C2, N3)	166 ± 42	153
χ_{CYS} (N2, CA2, CB2, SG2)	-124 ± 15	−46
φ_{GLY} (C2, N3, CA3, C3)	-75 ± 16, 154 ± 47	99

the S−H−O angle of the minimized GSH structure are similar to that observed in the atypical big cell C2 model where they are 4.0 Å and 125°, respectively. When the same procedure is performed after deprotonation of the −SH group, the minimized conformer (EMAS-GS^-) shows the sulfur atom at 3.1 Å from the oxygen atom (S−H−O angle = 134°), with a geometry compatible with a strong hydrogen bond interaction (Table 4 and Figure 4).

DISCUSSION

The above experiments represent the first investigation about the conformation of the GSH when it binds to GST P1-1 in solution and allow a useful comparison with the GSH structure observed in three different crystal forms refined to resolutions of 1.9 and 2.2 Å. The success of the TRNOE approach in determining the conformation of a small ligand bound to a large enzyme is critically related to the differentiation between direct and indirect NOE interactions. Comparison of TRNOESY and TRROESY experiments points out that no spin diffusion effects are detectable under our conditions. All conformers, compatible with TRNOESY data, show very similar and extended backbone conformation for the bound GSH which also superimposes well on the one found in all crystal complexes (Figure 3). Some differences have been observed for the geometry of the side-chain regions. The slight flexibility of the glycyl carboxylate (see Figure 3), may be apparent as this NMR technique is unable to detect fast exchangeable protons. In addition, the NMR data show the Gly residue to be well-defined and anchored to the protein; the intermolecular NOE observed at 3.76−7.35 ppm is likely due to this residue (and not to the CαH of Glu, see below) and may arise from the interaction between CαH of Gly and an aromatic proton at 7.35 ppm. This agrees with the short distance found in the normal crystal structure between the pseudoatom of the equivalent Cα protons of Gly and the ζ proton of Phe 8 (2.8 Å) or, alternatively, the ϵ1 (2.3 Å) or ζ2 (2.9 Å) protons of Trp 38. Therefore, this indicates that the orientation of the Gly residue of the bound GSH in the active site may be very similar to that found in the crystal complex. The alternative possibility that the intermolecular NOE at 3.76−7.35 ppm may be due to CαH proton of Glu is less probable; in fact, inspection of the X-ray derived complex structure shows the possible nearest protons at 3.41 or 4.32 Å (ϵ21 and ϵ22 of Gln 64), too far to give a quite strong intermolecular NOE. The different conformation of the Cys side chain is interesting. The geometry of the sulfhydryl group, as it appears in the normal crystal complex, is compatible with a hydrogen bond interaction between the sulfur atom of GSH and the hydroxyl group of Tyr 7 (Table 4). This aromatic residue is structurally conserved in all GSTs, except for the Theta isoenzyme, where the equivalent Tyr residue is probably replaced by a Ser residue (*10*). Its electrostatic interaction with the sulfur atom of GSH is crucial to lowering the pK_a of the bound GSH thiol group from 8.9 to 6.0−6.6 and also for a correct orientation of the thiol group into the active site (*47*). After modeling and restrained energy minimization in the crystallographic active site, this crucial hydrogen bond is not found for the representative un-ionized NMR conformer (DGSA-GSH); in fact, the GSH thiol group is about 4.0 Å away from the oxygen atom of Tyr 7 and with an unsuitable O−H−S angle (121°) (Table 4). A different geometry in solution is also suggested by an unexpected medium-strong NOE interaction between Cβ H of Cys-GSH and a proton at 1.23 ppm, which indicates a close enzyme proton within 3.0 Å, but, an inspection of the crystal structure reveals the closer possible protons to be the Cβ H and Cβ′H of Leu 52, away 4.28 and 5.79 Å, respectively. An explanation of the unusual geometry of −SH is the different ionization state of GSH in the two models. NMR experiments have been performed at pH 5.2, so the bound GSH is mainly un-ionized in the active site. In this form, the sulfur atom is a poor hydrogen-bonding proton acceptor, and its propensity to be oriented toward the hydroxyl group of Tyr 7 is quite low. When the NMR conformer is minimized into the active site by imposing the ionized form for the thiol group, the Cys side chain twists and the sulfur atom points toward the oxygen atom of Tyr 7 and is now in hydrogen

Table 4: Sulfhydryl Group Geometry of the Bound GSH

	DGSA-GSH[a]	EMAS-GSH[b]	EMAS-GS$^-$ [c]	X-ray-GSH[d]
rmsd (Å)	0.31	0.26	0.17	
χ_{CYS} (N2, CA2, CB2, SG2) (deg)	−118	−89	−63	−46
O−H−S angle (deg)	119	121	134	149
Tyr7−O···S−GSH distance	4.3	4.0	3.1	3.2

[a] Selected GSH NMR conformer (unionized) obtained by distance geometry-simulated annealing and positioned in the active site overlaying the backbone atoms to the crystal model. [b] DGSA-GSH after restrained energy minimization in the crystal binding site. [c] DGSA-GSH after deprotonation of the sulfhydryl group and restrained energy minimization in the crystal binding site. [d] Data refer to the normal crystal complex (small cell C2).

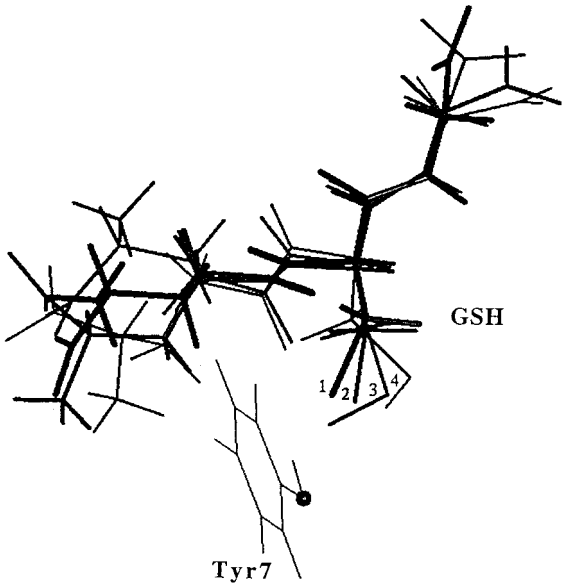

FIGURE 4: Relative orientation of the sulfhydryl group of bound GSH toward Tyr 7 in the GST P1-1 active site. In order of decreasing thickness: (1) structure of GSH in the normal crystal complex (small cell C2 form); (2) selected NMR structure of GSH in the ionized state after restrained energy minimization in the crystallographic binding site (EMAS-GS$^-$); (3) selected NMR structure in the un-ionized state after restrained energy minimization in the crystallographic binding site (EMAS-GSH); (4) selected NMR structure in the un-ionized state obtained by distance geometry-simulated annealing procedure and positioned in the active site overlaying the backbone atoms to the crystallographic model (DGSA-GSH).

bond distance (3.1 Å) and with a suitable O−H−S angle (134°) (see Figure 4, Table 4).

The conformation of GSH found in the atypical crystal also displays a different orientation of the thiol group in the active site. In fact, in this crystal form, grown at lower pH and temperature, the sulfur atom of GSH does not form a direct hydrogen bond with Tyr 7 (O−S distance = 4.0 Å and S−H−O angle = 125°), but it points away from this residue and the electrostatic interaction is mediated by a water molecule. Although we have no direct proof, it seems very likely that, under these conditions, GST P1-1 crystallized in complex with the un-ionized GSH.

In the crystal complex, the glutamyl moiety is stabilized by a number of hydrogen bonds and electrostatic interactions involving Arg 13, Gln 51, Gln 64, and Ser 65 of the same subunit and Asp 98 from the neighboring subunit. These interactions are identical with those found for *S*-hexylglutathione in the lower resolution (2.8 Å) crystal structure (*9*). Kinetic studies also indicated the γ-glutamyl site as the main binding determinant for GSH (*48*−*51*). The situation appears different in the NMR model. In fact the γ-glutamyl moiety

Scheme 1

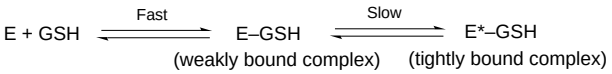

is poorly defined and thus appears highly flexible because there are not enough NOEs to define its structure. Exploration of the crystallographic G-site reveals that some protons of Arg 13, Gln 51, Pro 53, and Gln 64 are located within 3.0 Å from the CαH, CβH, and CγH of the glutamyl end. However, we detect only one single strong intermolecular NOE between CβH of Glu and a proton of the enzyme at 4.0 ppm but no possible protons with this chemical shift are located within 3.0 Å in the crystal structure. The lack of other intermolecular NOEs could possibly be due to the limits of our experimental conditions, but the presence of the strong NOE at 4.0 ppm suggests that in solution the glutamyl moiety could interact with the G-site in a different fashion. This unexpected finding may be the consequence of a multistep binding mechanism as shown in Scheme 1.

The existence of such a two-step binding mechanism has been suggested by preliminary time-resolved fluorescence data which show that, at saturating GSH concentrations, two families of GSH-GST P1-1 conformers exist at 20 °C. One of them (83%) is formed by a more rigid conformation of the G-site which could correspond to the tightly bound Michaelis complex, while the second one (17%) may be identified as the weakly bound precomplex showing a more flexible active site conformation (Stella et al., unpublished experiments). Pre-steady-state kinetic data also reveal a multistep binding mechanism in which a conformational transition of the precomplex into the tightly bound complex is rate limiting (*42*). Analysis of NOESY spectra for multistep binding systems has been discussed in detail (*52*). In the case of a three-state model for ligand−enzyme interaction, the conformation determined by TRNOESY may be related to the weakly bound complex if suitable values of kinetic constants for the binding process take place as well as pertinent cross-relaxation rates occur (*52*). At 5 °C, the values of the apparent rate constants for the precomplex formation and dissociation are $k_{on} \geq 10^6$ M^{-1} s^{-1} and $k_{off} \geq 1250$ s^{-1}, respectively. Moreover, the apparent rate constants for the reversible formation of the tightly bound complex are $k_2 = 1000$ s^{-1} and $k_{-2} = 34$ s^{-1}. By assuming a k_{on} value of 10^7−10^8 M^{-1} s^{-1}, as observed for most of the enzyme−substrate binding mechanisms (*53*), it follows that k_{off} should be 10^4−10^5 s^{-1}. By comparing k_{off} and k_{-2} with the estimated cross-relaxation rates for the bound GSH (0.15−15 s^{-1}), then both the tightly and the weakly bound forms could be detected by the TRNOESY approach and the NMR derived conformation may be a weighted average of the two possible bound conformations (52). However,

under our conditions, the population of free GSH which retains the magnetization of the precomplex is at least 10−100-fold higher than the population which reflects the magnetization of the tightly bound form. This suggests that our NMR data show a snapshot of the bound GSH mainly in the precomplex. In conclusion, in this early stage of binding, the glutamyl end appears to interact with the G-site differently from that seen in the tightly bound complex. New crystal structures with glutamyl modified GSH analogues (which simulate the precomplex conformation of the G-site) and NMR studies will lead the application of the complete relaxation and conformational exchange matrix analysis (CORCEMA) (*52*, *54*) of NOESY spectra which will better define the GSH conformation and its intermolecular contacts in the precomplex.

ACKNOWLEDGMENT

Fabio Bertocchi is acknowledged for the skillful technical assistance in the NMR experiments. We are indebted to an anonymous Reviewer for his/her helpful suggestions.

REFERENCES

1. Jakoby, W. B., and Habig, W. H. (1980) in *Enzymatic Basis of Detoxification* (Jakoby, W. B., Ed.) Vol. 2, pp 63−94, Academic Press, New York.
2. Mannervik, B., Alin, P., Guthenberg, C., Jensson, H., Tahir, M. K., Warholm, M., and Jörnvall, H. (1985) *Proc. Natl. Acad. Sci. U.S.A. 82*, 7202−7206.
3. Meyer, D. J., Coles, B., Pemble S. E., Gilmore, K. S., Fraser, G. M., and Ketterer, B. (1991) *Biochem. J. 274*, 409−414.
4. Buetler, T. M., and Eaton, D. L. (1992) *Environ. Carcinog. Ecotoxicol. Rev. 10*, 181−203.
5. Meyer, D. J., and Thomas, M. (1995) *Biochem. J. 311*, 739−742.
6. Sinning, I., Kleywegt, G. J., Cowan, S. W., Reinemer, P., Dirr, H. W., Huber, R., Gilliland, G. L., Armstrong, R. N., Ji, X., Board, P. G., Olin, B., Mannervik, B., and Jones, T. A. (1993) *J. Mol. Biol. 232*, 192−212.
7. Ji, X., Zhang, P., Armstrong, R. N., and Gilliland, G. L. (1992) *Biochemistry 31*, 10169−10184.
8. Reinemer, P., Dirr, H. W., Ladenstein, R., Schaffer, J., Gallay, O., and Huber, R. (1991) *EMBO J. 10*, 1997−2005.
9. Reinemer, P., Dirr, H. W., Ladenstein, R., Huber, R., Lo Bello, M., Federici, G., and Parker, M. W. (1992) *J. Mol. Biol. 227*, 214−226.
10. Wilce, M. C. J., Board, P. G., Feil, S. C., and Parker, M. W. (1995) *EMBO J. 14*, 2133-2143.
11. Ji, X., von Rosenvinge, E. C., Johnson, W. W., Tomarev, S. I., Piatigorsky, J., Armstrong, R. N., and Gilliland, G. L. (1995) *Biochemistry 34*, 5317−5328.
12. Ricci, G., Caccuri, A. M., Lo Bello, M., Rosato, N., Mei, G., Nicotra, M., Chiessi, E., Mazzetti, A. P., and Federici, G. (1996) *J. Biol. Chem. 271*, 16187−16192.
13. Batist, G., Tulpule, A., Sinha, B. K., Katki, A. G., Myers, C. E., and Cowan, K. H. (1986) *J. Biol. Chem. 261*, 15544−15549.
14. Black, S. M., Beggs, J. D., Hayes, J. D., Bartoszek, A., Muramatsu, M., Sakai, M., and Wolf, C. R. (1990) *Biochem. J. 268*, 309−315.
15. Puchalski, R., and Fahl, W. E. (1990) *Proc. Natl. Acad. Sci. U.S.A. 87*, 2443−2447.
16. Ni, F. (1994) *Prog. Nucl. Magn. Reson. Spectrosc. 26*, 517.
17. York, M. J., Beilharz, G. R., and Kuchel, P. W. (1987) *Int. J. Pept. Protein Res. 29*, 638−646.
18. Lo Bello, M., Battistoni, A., Mazzetti, A. P., Board, P. G., Muramatsu, M., Federici, G., and Ricci, G. (1995) *J. Biol. Chem. 270*, 1249−1253.
19. Ricci, G., Del Boccio, G., Pennelli, A., Lo Bello, M., Petruzzelli, R., Caccuri, A. M., Barra, D., and Federici, G. (1991) *J. Biol. Chem. 266*, 21409−21415.
20. Marion, D., and Wüthrich, K. (1983) *Biochem. Biophys. Res. Commun. 113*, 967−974.
21. Braunschweiler, L., and Ernst, R. R. (1983) *J. Magn. Reson. 53*, 521−528.
22. Bax, A., and Davis, D. G. (1985) *J. Magn. Reson. 65*, 355−360.
23. Jeener, J., Meier, B. H., Bachman, P., and Ernst, R. R. (1979) *J. Chem. Phys. 71*, 4546−4553.
24. Bothner-By, A. A., Stephens, R. L., Lee, J., Warren, C. D., and Jeanloz, R. W. (1984) *J. Am. Chem. Soc. 106*, 811−813.
25. Griesinger, C., and Ernst, R. R. (1987) *J. Magn. Reson. 75*, 261−271.
26. Brünger, A. T. (1992) X-PLOR, version 3.1, Yale University press, New Haven, CT.
27. Oakley, A. J., Lo Bello, M., Battistoni, A., Ricci, G., Rossjohn, J., Villar, H. O., and Parker, M. W. (1997) *J. Mol. Biol. 274*, 84−100.
28. Lo Bello, M., Oakley, A. J., Battistoni, A., Mazzetti, A. P., Nuccetelli, M., Mazzarese, G., Rossjohn, J., Parker, M. W., and Ricci, G. (1997) *Biochemistry 36*, 6207−6217.
29. Oakley, A. J., Rossjohn, J., Lo Bello, M., Caccuri, A. M., Federici, G., and Parker, M. W. (1997) *Biochemistry 36*, 576−585.
30. Dirr, H., Reinemer, P., and Huber, R. (1994) *J. Mol. Biol. 243*, 72−92.
31. García-Sáez, I., Párraga, A., Phillips, M. F., Mantle, T. J., and Coll, M. (1994) *J. Mol. Biol. 237*, 298−314.
32. Cameron, A. D., Sinning, I., L′Hermite, G., Olin, B., Board, P. G., Mannervik, B., and Jones, T. A. (1995) *Structure 3*, 717−727.
33. Ji, X., Armstrong, R. N., and Gilliland, G. L. (1993) *Biochemistry 32*, 12949−12954.
34. Ji, X., Johnson, W. W., Sesay, M. A., Dickert, L., Prasad, S. M., Ammon, H. L., Armstrong, R. N., and Gilliland, G. L. (1994) *Biochemistry 33*, 1043−1052.
35. Raghunathan, S., Chandross, R. J., Kretsinger, R. H., Allison, T. J., Penington, C. J., and Rule, G. S. (1994) *J. Mol. Biol. 238*, 815−832.
36. Ji, X., von Rosenvinge, E. C., Johnson, W. W., Armstrong, R. N., and Gilliland, G. L. (1996) *Proc. Natl. Acad. Sci. U.S.A. 93*, 8208−8213.
37. Reinemer, P., Prade, L., Hof, P., Neuefeind, T., Huber, R., Zettl, R., Palme, K., Schell, J., Koelln, I., Bartunik, H. D., and Bieseler, B. (1996) *J. Mol. Biol. 255*, 289−309.
38. Lim, K., Ho, J. X., Keeling, K., Gilliland, G. L., Ji, X., Ruker, F., and Carter, D. C. (1994) *Protein Sci. 3*, 2233−2244.
39. Dirr, H., Reinemer, P., and Huber, R. (1994) *Eur. J. Biochem. 220*, 645−661.
40. Wilce, M. C. J., and Parker, M. W. (1994) *Biochim. Biophys. Acta 1205*, 1−18.
41. Rabenstein, D. L., and Keire, D. A. (1989) *Glutathione: Chemical, Biochemical and Medical Aspects* (Dolphin, D., Poulson, R., and Avramovic, O., Eds.) pp 67−101, Wiley-Interscience Publication, New York.
42. Caccuri, A. M., Lo Bello, M., Nuccetelli, M., Nicotra, M., Rossi, P., Antonini, G., Federici, G., and Ricci, G. (1998) *Biochemistry 37*, 3028−3034.
43. Clore, G. M., and Gronenborn, A. M. (1982) *J. Magn. Reson. 48*, 402−417.
44. Clore, G. M., and Gronenborn, A. M. (1983) *J. Magn. Reson. 53*, 423−442.
45. Arepalli, S. R., Glaudemans, C. P. J., Daves, G. D., Jr., Kovac, P., and Bax, A. (1995) *J. Magn. Reson., Ser. B 106*, 195−198.
46. Jackson, P. L., Moseley, H. N., and Krishna, N. R. (1995) *J. Magn. Reson., Ser. B 107*, 289−292.
47. Liu, S., Zhang, P., Xinhua, J., Johnson, W. W., Gilliland, G. L., and Armstrong, R. N. (1992) *J. Biol. Chem. 267*, 4296−4299.
48. Adang, A. E. P., Duindam, A. J. G., Brussee, J., Mulder, G. J., and van der Gen, A. (1988) *Biochem. J. 255*, 715−720.

49. Adang, A. E. P., Brussee, J., Meyer, D. J., Coles, B., Ketterer, B., van der Gen, A., and Mulder, G. J. (1988) *Biochem. J. 255*, 721−724.
50. Adang, A. E. P., Meyer, D. J., Brussee, J., van der Gen, A., Ketterer, B., and Mulder, G. J. (1989) *Biochem. J. 264*, 759−764.
51. Adang, A. E. P., Brussee, J., van der Gen, A., and Mulder, G. J. (1990) *Biochem. J. 269*, 47−54.
52. Moseley, H. N. B., Curto, E. V., and Krishna, N. R. (1995) *J. Magn. Reson., Ser. B 108*, 243−261.
53. Fersht, A. (1985) *Enzyme structure and mechanism*, 2nd ed., pp 150−151, Freman W. H. & Company, NY.
54. Moseley, H. N., Lee, W., Arrowsmith, C. H., and Krishna, N. R. (1997) *Biochemistry 36*, 5293−5299.

BI971902O